# Organism motility in an oxygenated shallow-marine environment 2.1 billion years ago

Abderrazak El Albani[a,1], M. Gabriela Mangano[b], Luis A. Buatois[b], Stefan Bengtson[c], Armelle Riboulleau[d], Andrey Bekker[e], Kurt Konhauser[f], Timothy Lyons[e], Claire Rollion-Bard[g], Olabode Bankole[a], Stellina Gwenaelle Lekele Baghekema[a], Alain Meunier[a], Alain Trentesaux[d], Arnaud Mazurier[a], Jeremie Aubineau[a], Claude Laforest[a], Claude Fontaine[a], Philippe Recourt[d], Ernest Chi Fru[h], Roberto Macchiarelli[i,j], Jean Yves Reynaud[d], François Gauthier-Lafaye[k], and Donald E. Canfield[l,1]

[a]Unité Mixte de Recherche (UMR), Centre National de la Recherche Scientifique (CNRS), IC2MP 7285, University of Poitiers, 86073 Poitiers, France; [b]Department of Geological Sciences, University of Saskatchewan, Saskatoon, SK S7N 5A5, Canada; [c]Department of Palaeobiology, Swedish Museum of Natural History, SE-104 05 Stockholm, Sweden; [d]UMR 8187 Laboratoire d'Océanologie et de Géosciences, CNRS, University of Lille, Université du Littoral-Côte-d'Opale, 59655 Villeneuve d'Ascq, France; [e]Department of Earth Sciences, University of California, Riverside, CA 92521; [f]Department of Earth and Atmospheric Sciences, University of Alberta, Edmonton, AB, T6G 2E3, Canada; [g]Institut de Physique du Globe de Paris, Sorbonne Paris Cité, Université Paris Diderot, UMR 7154 CNRS, F-75005 Paris, France; [h]Geomicrobiology/Biogeochemistry, School of Earth and Ocean Sciences, Cardiff University, CF10 3AT Cardiff, United Kingdom; [i]Unité de Formation Géosciences, Université de Poitiers, 86073 Poitiers, France; [j]UMR 7194 CNRS, Muséum National d'Histoire Naturelle, Paris, France; [k]Laboratoire d'Hydrologie et de Géochimie de Strasbourg, UMR 7517 CNRS, 67084, Université de Strasbourg, France; and [l]Department of Biology, Nordic Center for Earth Evolution, DK-5230 Odense M, Denmark

Contributed by Donald E. Canfield, December 22, 2018 (sent for review September 11, 2018; reviewed by Phoebe A. Cohen and Marc Laflamme)

**Evidence for macroscopic life in the Paleoproterozoic Era comes from 1.8 billion-year-old (Ga) compression fossils [Han TM, Runnegar B (1992) *Science* 257:232–235; Knoll et al. (2006) *Philos Trans R Soc Lond B* 361:1023–1038], Stirling biota [Bengtson S et al. (2007) *Paleobiology* 33:351–381], and large colonial organisms exhibiting signs of coordinated growth from the 2.1-Ga Francevillian series, Gabon. Here we report on pyritized string-shaped structures from the Francevillian Basin. Combined microscopic, microtomographic, geochemical, and sedimentologic analyses provide evidence for biogenicity, and syngenicity and suggest that the structures underwent fossilization during early diagenesis close to the sediment–water interface. The string-shaped structures are up to 6 mm across and extend up to 170 mm through the strata. Morphological and 3D tomographic reconstructions suggest that the producer may have been a multicellular or syncytial organism able to migrate laterally and vertically to reach food resources. A possible modern analog is the aggregation of amoeboid cells into a migratory slug phase in cellular slime molds at times of starvation. This unique ecologic window established in an oxygenated, shallow-marine environment represents an exceptional record of the biosphere following the crucial changes that occurred in the atmosphere and ocean in the aftermath of the great oxidation event (GOE).**

motility | Paleoproterozoic Era | oxygenation | Francevillian

The exquisitely preserved sediments of the Francevillian Series B (FB) Formation from southeastern Gabon were deposited in an oxygenated (1, 2) offshore to offshore-transition environment at 2,100 ± 30 million years ago (Ma) (3, 4). The deposits pass upwards into shallow water, stromatolitic dolostones, and dolomitic cherts of the Francevillian C (FC) Formation (*SI Appendix*, Figs. S1 and S2), recording a regression (1, 2). The specimens for this study were collected from black, silty shale intercalated with siltstone to very fine-grained sandstone in the $FB_2$ Member of the FB Formation (*SI Appendix*, Figs. S1 and S2).

The black, silty shales preserve millimeter-sized, diverse string-shaped structures (Figs. 1 and 2), most of which are pyritized. These structures occur throughout the member; however, they are most abundant in the basal-most meter on the bedding plane (Fig. 1 and *SI Appendix*, Fig. S1*C*). Microbially induced sedimentary structures prevail in the interbedded sandstone and silty sandstone layers (*SI Appendix*, *Supplementary Information Text 1* and Fig. S3) and are commonly present in the vicinity of the string structures (Fig. 1 *E*, *F*, *I*, and *J*).

More than 80 specimens from several fossiliferous horizons were studied using X-ray microcomputed tomography (micro-CT) (Fig. 2, *SI Appendix*, Figs. S4–S7, and Movies S1–S4). The analysis reveals the presence of string-shaped structures within the strata (Fig. 2, *SI Appendix*, Figs. S4–S7, and Movies S1–S5). Some of these structures occur close to pyritized laminae lenses extending over several centimeters (Fig. 2 *C*–*F* and Movies S1–S3), suggesting an association with organic-rich mats where microbial sulfate reduction was enhanced (Fig. 2 *C*–*F* and *SI Appendix*, Figs. S3 and S5–S7). In one case, a sheetlike structure with a distinct boundary forms an apparent continuity with an equally distinct string (Fig. 3). Strings are mostly parallel to the bedding plane and, when observed in vertical cross sections (Fig. 2 *C*–*F*, *SI Appendix*, Fig. S6, and Movies S1 and S2), display an elliptic to rounded section, flattened parallel to the bedding (Fig. 4 *C* and *E* and *SI Appendix*, Fig. S6). They appear to have only a minor impact on the original sedimentary fabric with the laminae generally bending around

## Significance

The 2.1 billion-year-old sedimentary strata contain exquisitely preserved fossils that provide an ecologic snapshot of the biota inhabiting an oxygenated shallow-marine environment. Most striking are the pyritized string-shaped structures, which suggest that the producer have been a multicellular or syncytial organism able to migrate laterally and vertically to reach for food resources. A modern analogue is the aggregation of amoeboid cells into a migratory slug phase in modern cellular slime molds during time of food starvation. While it remains uncertain whether the amoeboidlike organisms represent a failed experiment or a prelude to subsequent evolutionary innovations, they add to the growing record of comparatively complex life forms that existed more than a billion years before animals emerged in the late Neoproterozoic.

Author contributions: A.E.A. and D.E.C. designed research; A.E.A., M.G.M., L.A.B., S.B., A.R., A.B., K.K., T.L., and D.E.C. performed research; A.E.A., M.G.M., L.A.B., S.B., A.R., A.B., K.K., T.L., C.R.-B., O.B., S.G.L.B., A. Meunier, A.T., A. Mazurier, J.A., C.L., C.F., P.R., E.C.F., R.M., J.Y.R., and D.E.C. analyzed data; A.E.A., M.G.M., L.A.B., S.B., A.R., A.B., K.K., T.L., C.R.-B., A. Meunier, F.G.-L., and D.E.C. wrote the paper; and O.B., S.G.L.B., A.T., J.A., and C.L. contributed to the fieldwork.

Reviewers: P.A.C., Williams College; and M.L., University of Toronto Mississauga.

The authors declare no conflict of interest.



[1]To whom correspondence may be addressed. Email: abder.albani@univ-poitiers.fr or dec@biology.sdu.dk.

This article contains supporting information online at www.pnas.org/lookup/suppl/doi:10.1073/pnas.1815721116/-/DCSupplemental.

Published online February 11, 2019.

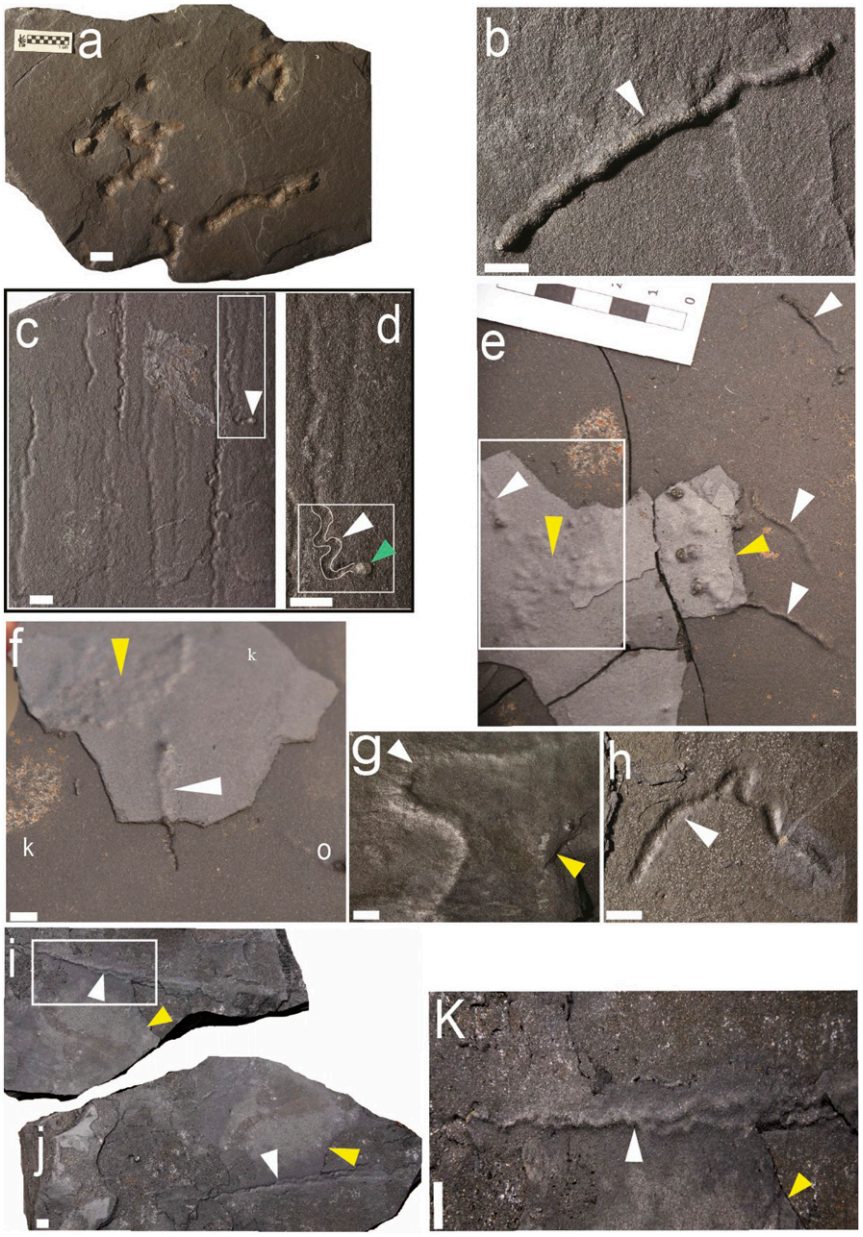


**Fig. 1.** Reflected-light photographs of pyritized string-shaped specimens from the Francevillian Series, Gabon. White and yellow arrows point to string-shaped specimens and microbial mats, respectively. (*A*) Slab displaying several straight specimens with straight to convoluted strings. (*B–I*) Sinuous strings. (*C*) Straight or slightly contorted strings; frame denotes specimen in *D*. (*D*) Enlarged part of *C*, contour of trace marked in white within frame. Note the termination of the trace showing a small pyrite globule (green arrow). (*E*) Slab displaying several subparallel specimens in the vicinity of bacterial mats. Note that the relief increase at the surface of the sediment from right to left for each specimen; frame denotes specimen in *F*. (*F*) Enlarged part of *E*, white arrow shows the detail of the trajectory of specimen under the fine clay laminae toward the bacterial mats (yellow arrow). (*I* and *J*) Part and counterpart of twinned contorted strings, parting from each other at upper white arrow; box denotes specimen in *K*. (*K*) Enlarged part of *J*; note the contorted strings and braided aspect. (Scale bars: 1 cm.)

these structures consistent with their early formation (Fig. 2*I*, *SI Appendix*, Figs. S6 and S7, and Movies S1 and S2). Specifically, the features indicate compaction of soft, fine-grained sediment around a relatively rigid object and show that the strings were in place and mineralized when the sediments were still compacting (Fig. 2*I*). Detrital phyllosilicate particles are parallel to bedding and aligned along the perimeter of the strings (Fig. 4). This relationship confirms precompactional formation of pyrite within the string structures resulting in local rearrangement of sediment grains during compaction. Combined SEM-back-scattered electron (BSE) imaging and energy-dispersive X-ray spectrometry (EDX) analyses also indicate contrasting textures and mineralogical compositions within and outside the strings (Fig. 4 *E* and *F*). Very few detrital minerals (e.g., quartz) are scattered within the pyrite strings, while authigenic illite and chlorite grains show signs of free growth within the pore spaces (Fig. 4 *E–G*).

The strings have a straight to sinuous shape (Figs. 1 and 2 and *SI Appendix*, Figs. S4–S8) and a maximum length of 170 mm. The simplest specimens are horizontal, unbranched, with straight (Figs. 1 *A* and *B* and 2 *A* and *B*, *SI Appendix*, Fig. S6, and Movie S3) to sinuous shapes (Fig. 1 *C–K*, *SI Appendix*, Figs. S6–S8, and Movies S1 and S2). They are 1–6 mm wide, with a relatively

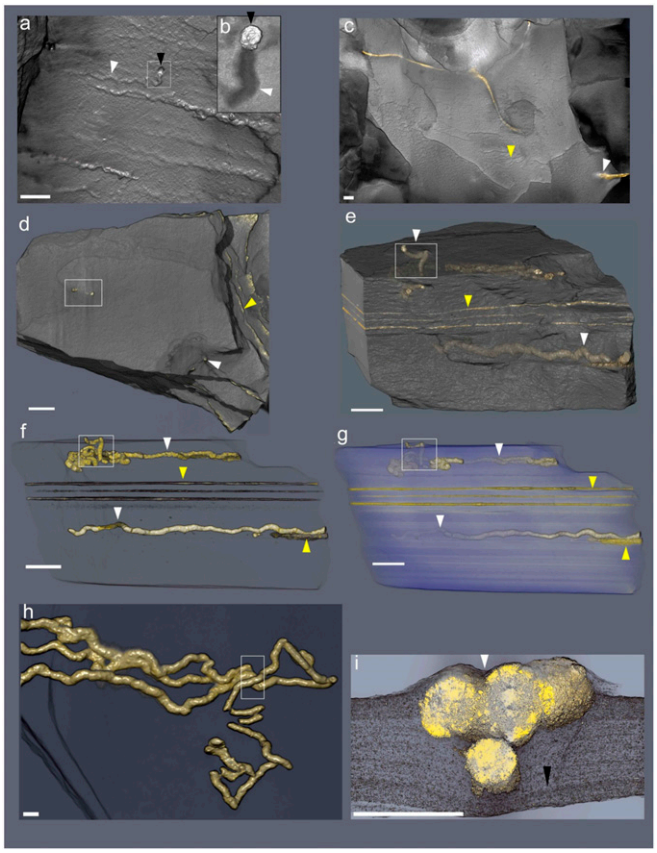


**Fig. 2.** Micro-CT-based reconstructions of string-shaped structures from the Francevillian Series, Gabon. White and yellow arrows point to string-shaped specimens and microbial mats, respectively. (*A*) Volume rendering showing the external surface of straight structures. *Inset* (*B*) shows enlargement of string ending with a pyrite crystal (black arrows). Same specimen as in Fig. 1 *D* and *E*. (*C*) External surface volume rendering showing weakly sinuous string. (*D*) External surface volume rendering, frame denotes the position of subvertical tubes. (*E*) External volume transparencies of the same specimen as in *D*, lateral view showing the string-shaped specimens inside the host rock. Frame denotes the position of subvertical tubes. (*F* and *G*) External volume transparencies of the same sample as in *D* and *E* at different heights in the sample. (*H*) Twinned contorted strings; box denotes portion (cross-section) figured in *I*. (*I*) Virtual cross-section of contorted strings, black arrow points to the precompactional deformation of silty shale laminae. (Scale bars: 1 cm.)

constant diameter along the structures (Fig. 2 *C*–*H* and Movie S3). A rounded termination is typically observed at the end of the structures (Figs. 1 and 2*A*), but one specimen ends with a spheroidal pyrite concretion showing a similar size to the string structure (Figs. 1 *C* and *D* and 2*A*, *Inset*). Specimens may develop a short, low-wavelength sinuosity and angular bends (Fig. 1 *D*, *C*, *I*, and *J*). In some cases, there are two or more parallel strings (Fig. 1 *C*, *D*, *I*, and *J*) that may intertwine and display a contorted helicoid shape, in places involving several strings in a braided pattern (Figs. 1 *I* and *J* and 2 *G* and *H*, *SI Appendix*, Fig. S4, and Movie S4). X-ray micro-CT and petrographic microscopy reveal that these string-shaped structures also intersect the stratification (Fig. 2*E*, *SI Appendix*, Figs. S7 and S8, and Movie S2). Strings might traverse silty-shale laminae and continue along at other levels, with angles of penetration ranging from 12° to 85° (Figs. 2 *D*–*F* and 4*E*, *SI Appendix*, Figs. S5*C* and S8, and Movies S1 and S2).

The pyritized string structures are present in sediment deposited under oxygenated bottom-water conditions (1, 5). This is consistent with the observation that selective pyritization preferably occurs in oxic, organic-lean sediments, because localized organic enrichments favor the needed chemical gradients. The pyrite structures display highly negative $\delta^{34}S$ values (−31‰ to −21‰; *SI Appendix*, Figs. S9 and S10 and Table S1), which are in the range of the lightest values for sedimentary pyrite deposited before the late Neoproterozoic Era (6, 7). Considering a $\delta^{34}S$ value of ∼15‰ for seawater sulfate at 2.1 Ga (6, 8–11), the low $\delta^{34}S$ values of the string-shaped structures indicate early diagenetic pyrite formation from sulfide generated by sulfate-reducing microorganisms close to the sediment–water interface from a relatively large seawater sulfate pool (12–14). Consistent with this observation, recent results suggest that concentration of sulfate in seawater may have been unusually high at this time, much higher than levels present immediately before and after this period of the Paleoproterozoic Era (12, 13).

The morphological patterns of the string-shaped structures and their relationship with the host sediment are very similar to those of burrows preserved through selective pyritization of mucus (14, 15), suggesting that the Francevillian structures may also be the result of early pyritization of a mucus strand. Nonetheless, it is critical to explore first the possibility of an abiogenic origin for the morphologies by making comparison with abiotic structures. Detailed comparison with syneresis cracks and pyrite precipitated from migrating fluids (*SI Appendix*, *Supplementary Information Text 2*, Fig. S11, and Table S2) indicates that the mineralogy, 3D morphology, texture, and sulfur isotope composition of the Francevillian string-shaped structures are markedly different from these abiogenic structures.

The pyritic strings described herein may sometimes look similar to other elongated body fossils in the Gabon biota, particularly where secondary pyritization has affected the morphology. Lobate body fossils previously reported from these beds in places may have a narrow, taillike appendix that in well-preserved specimens shows a flat cross-sectional profile and the same pattern of radiating fabric and transverse folding characteristic of the main body (14, 15). In heavily pyritized specimens, these primary features are obscured, resulting in featureless rods. These fossils resemble the specimen in Fig. 3 (see, e.g., figures 4C and D, 5, and 6E and F in ref. 5), but are usually coarser and display the typical fabric of the lobate fossils. Another fossil that may have similarity to string-shaped structures is a hitherto undescribed body fossil forming a network of interconnected rings, where the walls are expressed as thin pyritic strands along the bedding plane (*SI Appendix*, *Supplementary Information Text 3* and Fig. S12). Short fragments of this fossil missing the

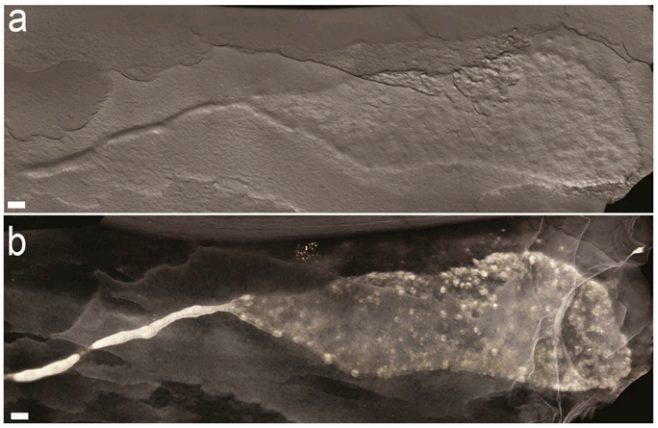


**Fig. 3.** (*A* and *B*) Volume rendering showing continuity between sheet and string morphologies in a single specimen. (Scale bars: 1 cm.)

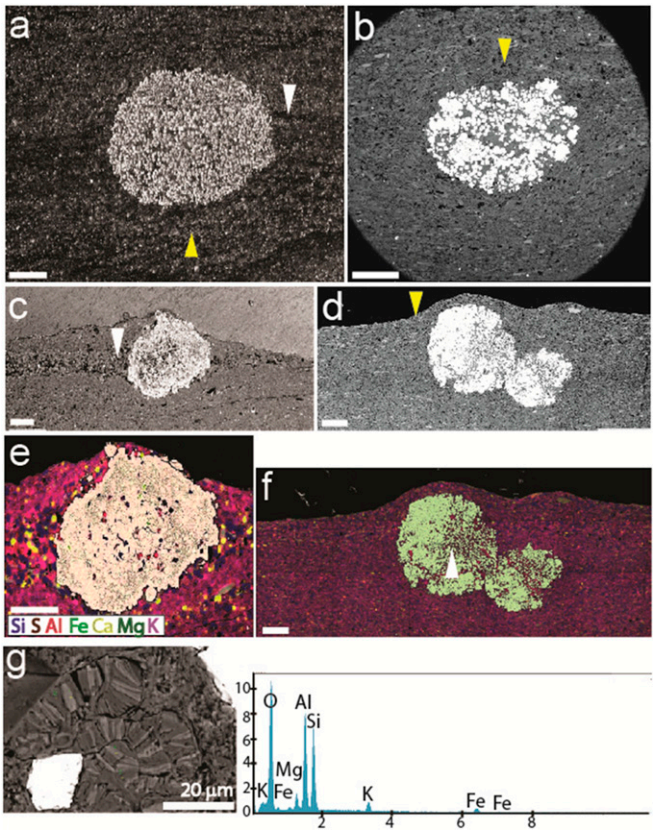


**Fig. 4.** Petrography with SEM and EDX of pyritized string-shaped structures from the Francevillian Series, Gabon. (*A* and *C*) Sediment laminae, white arrow, intersected by pyritic strings. Laminae bending around the pyrite string confirm precompactional formation, yellow arrow. (*B* and *D*) Bending of sediment layers, yellow arrows, around pyritic strings. (*E* and *F*) Element mapping of sections in *C* and *D*, showing mineralogical composition of the strings and embedding sediment. White arrow indicates the area of elemental point analyses (*G*). (Scale bars: 1 cm.) (*G*) Elemental points analysis indicate the presence of K, Mg, and Fe, which confirm the presence of illite and chlorite, respectively. The picture (*Left*) shows authigenic illite and chlorite grains and free growth of these minerals within the pore spaces.

branching points may be mistaken for the string structures on the bedding plane.

Experimental work (16) has shown that an oscillatory flow may interact with centimeter microbial aggregates, resulting in the formation on the sediment surface of elongate structures that may vaguely resemble the Francevillian string-shaped structures. However, the latter shows clear evidence of emplacement within the sediment. In addition, formation of the Francevillian Series B below the fair-weather wave base is inconsistent with continuous wave agitation.

A pyritized string of organic matter may represent the body of a filamentous organism or it may be the remnants of an organic tube or a mucus strand constructed by a motile organism. Among filamentous organisms, the closest living analogs to the Francevillian straight-to-sinuous structures are sulfur-oxidizing bacteria, such as *Thioploca* and *Beggiatoa*. These occur as horizontally to vertically oriented sheathed filaments or filament bundles in sediment, thriving at the interface between a weakly oxic sediment–water interface and underlying reducing sediments (17, 18). Individual filaments generally have a diameter of a few to tens of micrometers, although giant *Beggiatoa* filaments may reach nearly 200 µm in diameter (18). Sheathed *Thioploca* filaments bundles with up to 500-µm diameter have been recorded (17). The mucus sheaths of these sulfur-oxidizing bacteria allow filaments to migrate in the sediment between the surficial and the deeper portions (17). Importantly, these microbial structures are much smaller than ours. Phanerozoic pyritized organic trails and burrows of dimensions comparable to those of the Francevillian structures are commonly ascribed to animals (15, 19), but networks of pyritic filaments less than 1 mm in diameter have been interpreted as bacterial or fungal in origin (15).

Other than length differences, the distinction between pyritized tubes and trace fossils is subtle, but the latter can also be recognized by being massive and locally branching and through their incorporation of extraneous material (19–22). The Francevillian structures reported herein conform to this pattern and thereby resemble traces left by motile organisms, rather than individual filaments of bacteria or sheaths/tubes. They are somewhat reminiscent of simple straight forms resembling grazing trails in Ediacaran sedimentary successions, commonly in association with microbial mats (23–26). However, unlike these Ediacaran trails, the Francevillian structures have rounded terminations and occasional bulbous elements. Moreover, characteristic levees formed by sediment pushing on both sides, crucial in ascertaining the locomotory origin of some of the Ediacaran trace fossils, are absent in the Francevillian structures. In addition, a metazoan origin would not be supported by evidence from molecular clocks and the fossil record, which suggest a much younger origin for animals at ~650 Mya (23, 24).

Although the Francevillian specimens tend to be oriented parallel to bedding, they are occasionally oblique to subvertical in orientation, crossing up to 1.5 cm of sediment and locally disturbing primary laminations. These relationships can be taken as evidence for movement within the sediment, consistent with the absence of levees, which form in association with trails at the sediment–water interface, or even as tool marks produced by microbial aggregates moving under oscillating flow regimes (25). Given the inconsistencies with traces produced by animals or with sheaths enveloping motile bacteria, an alternative interpretation should be sought to explain their generation. Production by a microbial organism seems highly unlikely due to the lack of empirical evidence that such organism can produce megascopic infaunal trace fossils. There is no easy explanation, owing to morphologic simplicity of the structures and their great age, but a possible analog for the formation of these structures involves cellular slime molds, a group within Mycetozoa referred to as Dictyosteliida (27–29). These organisms, as illustrated by *Dictyostelium discoideum* and *D. polycephalum*, spend most of their life cycle as individual amoebae feeding on bacteria, but when food becomes scarce, single cells may aggregate to form a multicellular organism, referred to as "a slug," which subsequently moves on and within the sediment in search of a place for sporulation (29–32). During their aggregation stage, slime molds display behavior that is remarkably similar to that of simple animals (29).

The overall morphology of the Francevillian structures suggests an organism that was able to aggregate and migrate in a similar fashion to that of cellular slime molds, leaving a mucus trail behind. The occasional continuity between sheet and string morphology (Fig. 3) is particularly suggestive of this kind of behavior. The slug phase of cellular slime molds can develop differences in speed, with faster anterior relative to the posterior portion of the aggregate, resulting in a narrow isthmus between the anterior and posterior parts (33). The bulbous elements and the globular morphology of some of the string structures may have resulted from this movement pattern. Since metazoan trace fossils essentially reflect the maximum width of the producer, burrows tend to display constant diameter, but this is not necessarily the case with locomotive structures produced by mobile cell aggregates. The broken and crenulated appearance of some strings (Fig. 2 *E*–*G*) is consistent with slugs crossing over each other, resulting in the grafting of tips onto the slug as has been

observed in cellular slime molds during aggregation (33). In some cases, the tips of two slugs going in the same direction may fuse, producing a larger one. The tip of the aggregate may also split into two in a process known as twinning (33). In addition, parallel orientation of some structures may reflect parallel movement of the aggregates, as has been commonly observed in modern dictyostelid slugs that move along environmental gradients (30). The morphologic variability and intergradation of forms observed in the Francevillian structures (Fig. 1), in particular the transfiguration between sheets and strings (Fig. 3), as well as grafting and twinning of strings (Figs. 1 *I* and *J* and 2 *G* and *H* and *SI Appendix*, Fig. S4), suggest locomotion of cell aggregates rather than organisms having a distinct body shape and the presence of an interactive sensorial system that reflects deliberate behavior.

Structures consisting of pairs of ridges preserved in positive hyporelief in *Myxomitodes* of the 2.0–1.8 Ga Stirling biota have been interpreted as mucus-supported trails of syncytial or multicellular organisms comparable to dictyostelid slime molds (31). The Francevillian structures, which are up to ∼300 million years older than the Stirling biota, contrast with *Myxomitodes* in their shape and dimensions. Again, the Francevillian features were formed within the sediment as indicated by their oblique and subvertical orientations to sediment lamination and in association with matgrounds (Fig. 2 *C*–*G*), whereas *Myxomitodes* is exclusively parallel to the bedding and interpreted as having been formed at the sediment–water interface (31).

Regardless of the difficulties in distinguishing between body and trace fossils, the interpretation of the Francevillian structures as those produced by organisms comparable in behavior to cellular slime molds is consistent with their morphologic variability and mode of occurrence. The stimulus to become multicellular for dictyostelids is the lack of food (29–32).

Thus, the aggregative stage of slime molds could take place when all available organic material has been consumed. The Francevillian structures tend to occur next to matgrounds (Fig. 2 *C*–*F*), which are abundant and regularly spaced vertically. A plausible ecosystem structure includes a community of single (nonaggregated), amoebalike organisms thriving on buried microbial mats, but aggregating during times of starvation to move within the sediment to reach another mat at a different level. This mode of existence is consistent with movement guided by chemotaxis, which has been documented in modern dictyostelid slugs (33, 34). Slime molds have been observed to move vertically through sediment layers that are up to 7 cm thick (29, 30), showing the capability to penetrate the substrate in a way analogous to a muscular organism. This pattern is consistent with the localized vertical displacement revealed by the Francevillian structures. In addition, very shallow matgrounds could have enhanced oxygen concentrations creating oases rich in oxygen within the sediment at depths shallow enough to still receive light (32) (*SI Appendix*, *Supplementary Information Text 1*). Modern studies have shown that during the day, concentrations of oxygen within biomats can be up to 4 times higher than in the oxygen-stressed overlying water column, highlighting the role of biomats as both oxygen and food resource during the Precambrian (32).

However, there are two significant differences between the Francevillian structures and those formed by modern slime molds. First, slime molds live in soils, not in marine sediment (33). In open-marine environments, the chemical gradients that are necessary for the amoeboid cells to aggregate are not observed at the surface of sediments, but frequently develop within the sediment as a result of microbial activity and sediment permeability. This argument is strong in rejecting a slime-mold interpretation in the case of the surface trace *Myxomitodes* (31). Unlike *Myxomitodes*, the Francevillian structures were formed within a fine-grained and overall undisturbed sediment, where the development of chemical gradients was favored. Second, the width of modern slime-mold slugs is up to 0.2 mm, significantly smaller than that of the structures documented here. Importantly, we are not suggesting that the Francevillian structures were produced by slime molds, although the size and complexity of the fossils suggest that the organism may have been a eukaryote. We rather advocate an analogous situation wherein amoebalike organisms with the capability to aggregate in a similar fashion could have been responsible for producing these complex structures. The restriction of modern dictyostelids to soils does not rule out the possibility that amoebalike organisms may have been able to evolve the trait of aggregation in marine environments below the sediment–water interface, particularly in microbially bound sediments.

The timing of origin of eukaryotes and its potential link to the GOE has been the focus of intense debate (35–37). Integration of genomic and fossil evidence suggests that eukaryotes emerged ∼1.84 Ga ago, therefore postdating the GOE (37) and the Francevillian structures, which correspond in age to the end of the Lomagundi Event (∼2.22–2.06 Ga). This event represents the largest global positive C isotope excursion in Earth's history, which is recorded in the FB and FC formations of the Francevillian Series (2). This excursion is thought to reflect a time of relatively high oxygen content in the atmosphere and ocean relative to the time intervals immediately before and after (38). Regardless of the ∼300 My discrepancy between the Francevillian and the proposed timing for origin of eukaryotes, it is reasonable to assume that such an increase in oxygenation may have promoted evolutionary innovations, such as those recorded by the Gabonese biota and associated ecosystems (1, 39).

The Lomagundi Event may have ended up with a dramatic deoxygenation after which seawater $O_2$ levels remained near or below the lower limit necessary for complex life to survive until the late Neoproterozoic (40). In addition to this broad temporal relationship with an oxygen increase, the FB and FC formations were deposited in nearshore to offshore environments that allowed widespread development of microbial mats (*SI Appendix*, Fig. S3). These shallow-water, oxygen and food-rich conditions within the photic zone were instrumental for the establishment of an ecosystem able to harbor more advanced forms of life, including organisms that could migrate. The fossiliferous Francevillian strata were ultimately preserved in essentially undeformed and nonmetamorphosed strata (41). These special conditions underscore the uniqueness of the Francevillian biota, although it cannot be entirely excluded that our occurrence is related more to favorable taphonomic conditions than to environmental or evolutionary drivers/patterns. While it remains uncertain whether the Francevillian string-shaped structures represent a failed experiment or a prelude to subsequent evolutionary innovations, they add to the growing record of comparatively more complex life forms that colonized shallow-marine environments more than a billion years before animals emerged in the late Neoproterozoic.

## Methods

Textural relationships between the pyritized string-shaped structures and the silty shale matrix embedding the structures were assessed on polished slab sections with a ZEISS Discovery V8 stereoscope combined with AxioCam ERc 5s microscope camera. SEM was carried out on a JEOL 5600 LV equipped with an Oxford EDX for mineralogical analyses.

The micro-CT analysis of the samples was run on an RX-solutions EasyTom XL Duo equipment, which has one micro- and one nanofocus (LaB6 filament) Hamamatsu X-ray sources coupled to a Varian PaxScan 2520DX flat panel. Reconstructions were done with the XAct software (RX-solutions) with a classical filtered back projection algorithm and reduction of beam hardening artifact. Virtual sections, 3D rendering, and videos were performed with Avizo Fire v.9.2 (FEI).

Values of $\delta^{34}S$ were measured with secondary ion mass spectrometry (SIMS) using a Cameca IMS1270 and 1280 at Centre de Recherches Pétrographiques et Géochimiques facility (Nancy, France). The sulfur isotope compositions were

measured using a 20-μm $Cs^+$ primary beam of ∼2–5 nA. Sulfur isotopes were measured in a multicollection mode using two off-axis Faraday cups (L′2 and H1). The gains of the Faraday cups were intercalibrated at the beginning of the analytical session and their offsets were determined before each analysis during the presputtering (300 s). Typical ion intensities of $3 \times 10^9$ counts per second were obtained on $^{32}S^-$, so that an internal error better than ±0.1‰ can be reached. Instrumental mass fractionation and external reproducibility were determined by multiple measurements of the in-house reference material Pyr3B ($\delta^{34}S = +1.41‰$). The external reproducibility ranges between 0.05 and 0.40‰ (1 sigma) depending on the analytical session.

**ACKNOWLEDGMENTS.** For information and scientific discussion, we thank, P.-D. Mouguiama, F. D. Idiata, L. White, J. C. Baloche, R. Oslisly, F. Weber, A. Chirazi, F. Pambo, Idalina Moubiya Mouélé, and J. L. Albert. For assistance, we acknowledge C. Lebailly, Ph. Jalladeau, D. Autain, and S. Riffaut and the administrative staff of the University of Poitiers. We appreciate assistance from the Gabonese government, Centre National Pour la Recherche Scientifique & Technique du Gabon (CENAREST), General Direction of Mines and Geology of Gabon, Sylvia Bongo Ondimba Foundation, Agence Nationale des Parcs Nationaux du Gabon, University of Masuku, COMILOG and SOCOBA Companies, French Embassy at Libreville, Institut Français du Gabon, Le Centre National de la Recherche Scientifique (CNRS), and La Région Nouvelle Aquitaine for their supports. The authors acknowledge the support from RX-Solutions (Industrial X-Ray Tomography company), the Trace Analysis for Chemical, Earth and Environmental Sciences (TrACEES) platform from the Melbourne Collaborative Infrastructure Research Program at the University of Melbourne and P′ Institute UPR 3346 from Poitiers University.

1. El Albani A, et al. (2010) Large colonial organisms with coordinated growth in oxygenated environments 2.1 Gyr ago. *Nature* 466:100–104.
2. Canfield DE, et al. (2013) Oxygen dynamics in the aftermath of the Great Oxidation of Earth's atmosphere. *Proc Natl Acad Sci USA* 110:16736–16741.
3. Bros R, Stille P, Gauthier-Lafaye F, Weber F, Clauer N (1992) Sm-Nd isotopic dating of Proterozoic clay material: An example from the Francevillian sedimentary series, Gabon. *Earth Planet Sci Lett* 113:207–218.
4. Horie K, Hidaka H, Gauthier-Lafaye F (2005) U-Pb geochronology and geochemistry of zircon from the Franceville series at Bidoudouma, Gabon. *Geochim Cosmochim Acta* 69:A11.
5. El Albani A, et al. (2014) The 2.1 Ga old Francevillian biota: Biogenicity, taphonomy and biodiversity. *PLoS One* 9:e99438.
6. Canfield DE, Farquhar J (2009) Animal evolution, bioturbation, and the sulfate concentration of the oceans. *Proc Natl Acad Sci USA* 106:8123–8127.
7. Zhelezinskaia I, Kaufman AJ, Farquhar J, Cliff J (2014) Large sulfur isotope fractionations associated with Neoarchean microbial sulfate reduction. *Science* 346:742–744.
8. Guo Q, et al. (2009) Reconstructing Earth's surface oxidation across the Archean-Proterozoic transition. *Geology* 37:399–402.
9. Canfield DE (2001) Isotope fractionation by natural populations of sulfate-reducing bacteria. *Geochim Cosmochim Acta* 65:1117–1124.
10. Habicht KS, Gade M, Thamdrup B, Berg P, Canfield DE (2002) Calibration of sulfate levels in the archean ocean. *Science* 298:2372–2374.
11. Johnston DT, Farquhar J, Canfield DE (2007) Sulfur isotope insights into microbial sulfate reduction: When microbes meet models. *Geochim Cosmochim Acta* 71: 3929–3947.
12. Planavsky NJ, Bekker A, Hofmann A, Owens JD, Lyons TW (2012) Sulfur record of rising and falling marine oxygen and sulfate levels during the Lomagundi event. *Proc Natl Acad Sci USA* 109:18300–18305.
13. Scott C, et al. (2014) Pyrite multiple-sulfur isotope evidence for rapid expansion and contraction of the early Paleoproterozoic seawater sulfate reservoir. *Earth Planet Sci Lett* 389:95–104.
14. Schieber J (2002) The role of an organic slime matrix in the formation of pyritized burrow trails and pyrite concretions. *Palaios* 17:104–109.
15. Virtasalo JJ, Löwemark L, Papunen H, Kotilainen AT, Whitehouse MJ (2010) Pyritic and baritic burrows and microbial filaments in postglacial lacustrine clays in the northern Baltic Sea. *J Geol Soc London* 167:1185–1198.
16. Mariotti G, Pruss SB, Ai X, Perron JT, Bosak T (2016) Microbial origin of early animal trace fossils? *J Sediment Res* 86:287–293.
17. Jørgensen BB, Gallardo VA (1999) *Thioploca* spp.: Filamentous sulfur bacteria with nitrate vacuoles. *FEMS Microbiol Ecol* 28:301–313.
18. Larkin J, Henk MC, Aharon P (1994) *Beggiatoa* in microbial mats at hydrocarbon vents in the Gulf of Mexico and Warm Mineral Springs, Florida. *Geo Mar Lett* 14:97–103.
19. Thomsen E, Vorren TO (1984) Pyritization of tubes and burrows from Late Pleistocene continental shelf sediments off North Norway. *Sedimentology* 31:481–492.
20. Seilacher A, Buatois LA, Mángano MG (2005) Trace fossils in the Ediacaran–Cambrian transition: Behavioral diversification, ecological turnover and environmental shift. *Palaeogeogr Palaeoclimatol Palaeoecol* 227:323–356.
21. Jensen S, Droser ML, Gehling JG (2006) A critical look at the Ediacaran trace fossil record. *Neoproterozoic Geobiology and Paleobiology*, eds Xiao S, Kaufman AJ (Springer, Dordrecht, The Netherlands), pp 115–157.
22. Buatois LA, Mángano MG (2016) Ediacaran ecosystems and the dawn of animals. *The Trace-Fossil Record of Major Evolutionary Events: Volume 1: Precambrian and Paleozoic*, eds Mángano MG, Buatois LA (Springer, Dordrecht, The Netherlands), pp 27–72.
23. Cunningham JA, Liu AG, Bengtson S, Donoghue PCJ (2017) The origin of animals: Can molecular clocks and the fossil record be reconciled? *BioEssays* 39:1–12.
24. Love GD, et al. (2009) Fossil steroids record the appearance of Demospongiae during the Cryogenian period. *Nature* 457:718–721.
25. Mariotti G, Pruss SB, Perron JT, Bosak T (2016) Microbial shaping of sedimentary wrinkle structures. *Nat Geosci* 7:736–740.
26. Hagiwara H (1991) A new species and some new records of dictyostelid cellular slime molds from Oman. *Bull Natl Sci Mus Tokyo Ser B* 17:109–121.
27. Wallraff E, Wallraff HG (1997) Migration and bidirectional phototaxis in *Dictyostelium discoideum* slugs lacking the actin cross-linking 120 kDa gelation factor. *J Exp Biol* 200:3213–3220.
28. Sternfeld J, O'Mara R (2005) Aerial migration of the Dictyostelium slug. *Dev Growth Differ* 47:49–58.
29. Bonner JT (2006) Migration in *Dictyostelium polycephalum*. *Mycologia* 98:260–264.
30. Bonner JT, Lamont DS (2005) Behavior of cellular slime molds in the soil. *Mycologia* 97:178–184.
31. Bengtson S, Rasmussen B, Krapež B (2007) The Paleoproterozoic megascopic Stirling biota. *Paleobiology* 33:351–381.
32. Gingras M, et al. (2011) Possible evolution of mobile animals in association with microbial mats. *Nat Geosci* 4:372–375.
33. Kessin RH (2001) *Dictyostelium: Evolution, Cell Biology, and the Development of Multicellularity* (Cambridge Univ Press, Cambridge, United Kingdom).
34. Bonner JT (2009) *The Social Amoebae: The Biology of Cellular Slime Molds* (Princeton Univ Press).
35. Schirrmeister BE, de Vos JM, Antonelli A, Bagheri HC (2013) Evolution of multicellularity coincided with increased diversification of cyanobacteria and the Great Oxidation Event. *Proc Natl Acad Sci USA* 110:1791–1796.
36. Knoll AH, Nowak MA (2017) The timetable of evolution. *Sci Adv* 3:e1603076.
37. Betts HC, et al. (2018) Integrated genomic and fossil evidence illuminates life's early evolution and eukaryote origin. *Nat Ecol Evol* 2:1556–1562.
38. Lyons TW, Reinhard CT, Planavsky NJ (2014) The rise of oxygen in Earth's early ocean and atmosphere. *Nature* 506:307–315.
39. Aubineau J, et al. (2018) Unusual microbial mat-related structural diversity at 2.1 billion years old and implications for the Francevillian biota. *Geobiology* 16:476–497.
40. Planavsky NJ, et al. (2014) Earth history. Low mid-Proterozoic atmospheric oxygen levels and the delayed rise of animals. *Science* 346:635–638.
41. Gauthier-Lafaye F, Weber F (2003) Natural nuclear fission reactors: Time constraints for occurrence, and their relation to uranium and manganese deposits and to the evolution of the atmosphere. *Precambrian Res* 120:81–100.